This document is downloaded from DR-NTU, Nanyang Technological University Library, Singapore.

Title	Broadly tunable one-way terahertz plasmonic waveguide based on nonreciprocal surface magneto plasmons
Author(s)	Hu, Bin; Wang, Qi Jie; Zhang, Ying
Citation	Hu, B., Wang, Q. J., & Zhang, Y. (2012). Broadly tunable one-way terahertz plasmonic waveguide based on nonreciprocal surface magneto plasmons. Optics Letter, 37(11), 1895-1897.
Date	2012
URL	http://hdl.handle.net/10220/10972
Rights	© 2012 Optical Society of America. This paper was published in Optics Letter and is made available as an electronic reprint (preprint) with permission of Optical Society of America. The paper can be found at the following official DOI: [http://dx.doi.org/10.1364/OL.37.001895]. One print or electronic copy may be made for personal use only. Systematic or multiple reproduction, distribution to multiple locations via electronic or other means, duplication of any material in this paper for a fee or for commercial purposes, or modification of the content of the paper is prohibited and is subject to penalties under law.

Broadly tunable one-way terahertz plasmonic waveguide based on nonreciprocal surface magneto plasmons

Bin Hu,[1] Qi Jie Wang,[1,2,*] and Ying Zhang[3]

[1]*Division of Microelectronics, School of Electrical and Electronic Engineering, Nanyang Technological University, 50 Nanyang Avenue, 639798, Singapore*

[2]*Division of Physics and Applied Physics, School of Physical and Mathematical Sciences, Nanyang Technological University, 637371, Singapore*

[3]*Singapore Institute of Manufacturing Technology, 71 Nanyang Drive, 638075 Singapore*

**Corresponding author: qjwang@ntu.edu.sg*

Received October 13, 2011; revised April 9, 2012; accepted April 9, 2012; posted April 9, 2012 (Doc. ID 156431); published May 23, 2012

One-way-propagating broadly tunable terahertz plasmonic waveguide at a subwavelength scale is proposed based on a metal–dielectric–semiconductor structure. Unlike other one-way plasmonic devices that are based on interference effects of surface plasmons, the proposed one-way device is based on nonreciprocal surface magneto plasmons under an external magnetic field. Theoretical and simulation results demonstrate that the one-way-propagating frequency band can be broadly tuned by the external magnetic fields. The proposed concept can be used to realize various high performance tunable plasmonic devices such as isolators, switches and splitters for ultracompact integrated plasmonic circuits. © 2012 Optical Society of America

OCIS codes: 240.6680, 230.7380, 230.1360, 230.3810.

Rapid development in terahertz (THz) science and technology has been made in recent years because of huge potential in imaging, spectroscopy, biomedical sciences, and integrated circuits [1–3]. For those applications, THz plasmonic components, e.g., waveguides, based on surface plasmons (SPs) or spoof surface plasmons have been proposed due to the sub-wavelength confinement for miniaturized devices [4,5]. However, these plasmonic waveguides are two-way waveguides; i.e., light waves propagate in both the forward and the backward directions. One-way-propagating waveguides are of particular importance for functional devices such as isolators, switches and splitters.

So far, most one-way-propagating plasmonic devices have been proposed based on interference of SPs [6,7]. This effect is strongly sensitive to geometric structure variations, making the fabrication of such devices very difficult. Another approach is to use the nonreciprocal effect of SPs under an external magnetic field (MF) [also called surface magneto plasmons (SMPs)] [8]. The dispersions of the forward- and backward-propagating SMPs terminate at different cut-off frequencies, making it possible to realize an absolute one-way plasmonic waveguide [9]. However, this device [9] is only applicable in the visible frequencies, and the required MF is too strong to be realized ($B > 10^3$ T). It is noted that the largest achievable MFs is $\sim 10^2$ T.

In this Letter, we propose a simple THz one-way subwavelength plasmonic waveguide that needs only 1 T. By tuning the applied MF, we find through both theoretical analyses and numerical simulations that the central frequency of the one-way-propagating frequency band can be broadly tuned from 1.5 to 0.36 THz when the MF increases from 0.5 to 5 T. In addition, the bandwidth of the one-way-propagating frequency band can be broadened by using a dielectric material with a higher permittivity in the proposed structure. As illustrative examples, we demonstrate a one-way THz plasmonic isolator with an extinction ratio of 100% and a tunable THz plasmonic switch.

The schematic structure of the proposed waveguide is composed of a metal-dielectric-semiconductor structure as depicted in Fig. 1(a). The metal and the semiconductor layers are half-infinite, and the thickness of the dielectric layer is denoted by w. A TM-polarized SMP (with the MF component parallel to the y axis) propagates along the z direction at the dielectric/metal and dielectric/semiconductor layers. The external static MF is applied uniformly on the whole structure along the y axis (as indicated by B), forming a Voigt configuration. The dielectric constants of both the metal and the semiconductor can be expressed by a tensor [10,11]:

$$\overleftrightarrow{\varepsilon} = \varepsilon_\infty \begin{bmatrix} \varepsilon_{xx} & 0 & \varepsilon_{xz} \\ 0 & \varepsilon_{yy} & 0 \\ -\varepsilon_{xz} & 0 & \varepsilon_{xx} \end{bmatrix}, \tag{1}$$

where in the lossless case, the parameters in Eq. (1) can be expressed as $\varepsilon_{xx} = 1 - \omega_p^2/(\omega^2 - \omega_c^2)$, $\varepsilon_{xz} = -i\omega_p^2\omega_c/[\omega(\omega^2 - \omega_c^2)]$, and $\varepsilon_{yy} = 1 - \omega_p^2/\omega^2$. Here ω is the angular

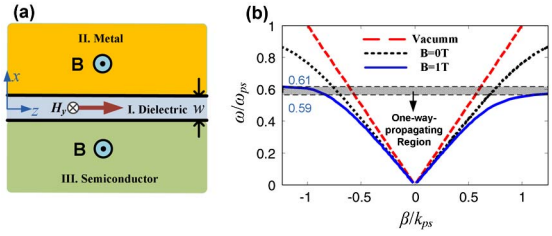

Fig. 1. (Color online) (a) Schematic structure of the one-way-propagating THz plasmonic waveguide. It is composed of metal (upper), dielectric (middle), and semiconductor (lower) layers. (b) Dispersion relations of the THz surface magneto plasmons without and with an external MF.

 © 2012 Optical Society of America

frequency of the incident wave, ω_p is the plasma frequency of metal or semiconductor (in the following, the plasma frequencies of the metal and the semiconductor are denoted by ω_{pm} and ω_{ps}, respectively), ε_∞ is the high-frequency permittivity, and $\omega_c = eB/m^*$ is the cyclotron frequency. e and m^* are the charge and the effective mass of electrons, respectively. It should be noted that ω_{ps} is in the order of $\sim 10^{13}$ Hz. When B is 1 T, the cyclotron frequency ($\omega_c \sim 10^{12}$) is comparable with ω_{ps}; thus the effect of the B can be observable. However, ω_{pm} is in the order of $\sim 10^{16}$ Hz, making B very large to observe the effect of the MF. Therefore, using semiconductors instead of metals can dramatically weaken the desired MFs. In THz frequency, due to $\omega_{pm} \gg \omega$, metals resemble perfect conductors [12] and can be regarded as isotropic, with a permittivity of $\varepsilon_m = \varepsilon_{m,xx}$. From the Maxwell equations and Eq. (1), the electromagnetic (EM) fields in the three layers can be expressed as

$$\begin{aligned}
H_y^{(II)} &= Ce^{-\kappa_2(x-w/2)},\\
E_z^{(II)} &= -\frac{i\kappa_2}{\omega\varepsilon_0\varepsilon_m}Ce^{-\kappa_2(x-w/2)},\\
H_y^{(I)} &= Ae^{-\kappa_1 x} + Be^{\kappa_1 x},\\
E_z^{(I)} &= -\frac{i\kappa_1}{\omega\varepsilon_0\varepsilon_d}(Ae^{-\kappa_1 x} - Be^{\kappa_1 x}),\\
H_y^{(III)} &= De^{\kappa_3(x+w/2)},\\
E_z^{(III)} &= \frac{i\beta\varepsilon_{s,xz}De^{\kappa_3(x+w/2)} - \varepsilon_{s,xx}\kappa_3 De^{\kappa_3(x+w/2)}}{i\omega\varepsilon_0(\varepsilon_{s,xx}^2 + \varepsilon_{s,xz}^2)},
\end{aligned} \tag{2}$$

where $\varepsilon_{s,ij}$ is the corresponding elements of permittivity tensor of the semiconductor; ε_d is the dielectric constant of the dielectric layer; A, B, C, and D are the amplitudes of the EM fields; and β is the propagation constant of the waveguide. κ_1, κ_2, and κ_3 are defined by $\kappa_1^2 = \beta^2 - k_0^2\varepsilon_d$, $\kappa_2^2 = \beta^2 - k_0^2\varepsilon_m$, $\kappa_3^2 = \beta^2 - k_0^2\varepsilon_s$, where $\varepsilon_s = \varepsilon_{s,xx} + \varepsilon_{s,xz}^2/\varepsilon_{s,xx}$ is the Voigt dielectric constant of the semiconductor [8]. Considering the continuity of H_y and E_z at the interfaces of the metal/dielectric and semiconductor/dielectric, we have the dispersion relation of the waveguide from Eq. (2):

$$\begin{aligned}
&\left\{\frac{\kappa_2\kappa_3}{\kappa_1^2}\frac{1}{\varepsilon_m\varepsilon_s} + \frac{1}{\varepsilon_d^2} - i\frac{\beta\kappa_2}{\kappa_1^2}\frac{\varepsilon_{s,xz}}{\varepsilon_m\varepsilon_s\varepsilon_{s,xx}}\right\}\tanh(\kappa_1 w)\\
&\quad + \left[\frac{\kappa_3}{\kappa_1}\frac{1}{\varepsilon_d\varepsilon_s} + \frac{\kappa_2}{\kappa_1}\frac{1}{\varepsilon_m\varepsilon_d} - i\frac{\beta}{\kappa_1}\frac{\varepsilon_{s,xz}}{\varepsilon_d\varepsilon_s\varepsilon_{s,xx}}\right] = 0.
\end{aligned} \tag{3}$$

The nonreciprocal effect can be seen clearly from Eq. (3), where the dispersion relation curves are different for $\beta > 0$ (SMPs propagating along the z direction) and $\beta < 0$ (SMPs propagating along the $-z$ direction). Without loss of generality, here we consider InSb, gold, and air as the semiconductor, metal, and dielectric materials in the calculation. The corresponding parameters of InSb at room temperature are given by $m^* = 0.014m_0$ (m_0 is the free electron mass in vacuum), $\omega_{ps} = 1.26 \times 10^{13}$ Hz, and $\varepsilon_\infty = 15.68$ [13]. $\omega_{pm} = 1.37 \times 10^{16}$ Hz [14]. The width of the waveguide is $w = 0.1\lambda_{ps}$, where λ_{ps} is the InSb plasma wavelength defined as $2\pi c/\omega_{ps}$. Figure 1(b) shows the dispersion curves of the forward- and backward-propagating THz SMPs waves with ($B = 1$ T) and without the external MFs in the frequency region $\omega/\omega_{ps} = [0, 1]$. It can be seen that without the MF, the dispersion curves are symmetric for both the forward- and backward-propagating waves, as shown in the black dotted lines. However, when MF is applied, the dispersion curves of the two propagating waves are different. The forward-propagating mode vanishes at a frequency of $\omega/\omega_{ps} = 0.59$, while the backward-propagating mode vanishes at a higher frequency of $\omega/\omega_{ps} = 0.61$. This means that the THz waves in the frequency region of $\omega/\omega_{ps} = [0.59, 0.61]$ (corresponding to $f = [1.18, 1.23]$ THz) can only propagate backward.

To verify the theoretical calculations, we conduct simulations with the finite element method (FEM) by using COMSOL Multiphysics. The results are plotted in Figs. 2(a)–2(d). Without the external MF, the field distributions of the forward- and backward-propagating waves are the same [see (a) and (b), respectively]. However, when 1 T MF is applied, the forward-propagating THz wave is blocked [see Fig. 2(c)], while the backward-propagating wave can still propagate through the slit [see Fig. 2(d)]. The reason for the results in Fig. 2(c) is that the forward-propagating SMP mode is blocked under the MF, thus SMPs cannot be excited by the edge diffractions [6] when the THz wave impinges on the slit. The transmitted intensity curves of the forward- and backward-propagating waves under the MF are depicted in Fig. 2(e). It can be seen that the one-way region is $\omega = [0.59, 0.612]\omega_{ps}$, which agrees very well with the theoretical results. In the simulations, we consider a slit with finite length of $L = 300$ μm. However, the one-way effect can also be observed for other slit lengths.

It is important to study the factors that affect the performance of the one-way-propagating frequency band. According to Eq. (3), we calculate the cutoff frequencies of the forward- (ω_{Vf}) and the backward- (ω_{Vb}) propagating modes versus the applied MFs and versus the permittivity of the dielectric layer, shown in Figs. 3(a) and 3(b), respectively. It is found that the external MF affects the

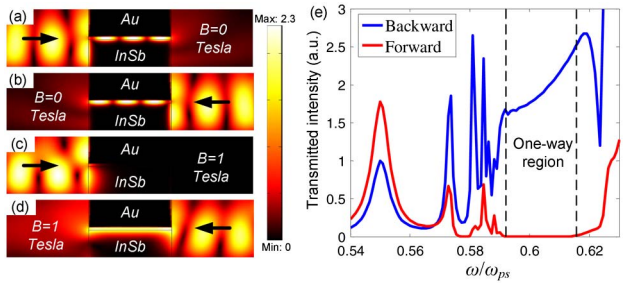

Fig. 2. (Color online) (a)–(d) Field distribution $|H_y|^2$ of the forward- and backward-propagating waves in a sub-wavelength slit with and without an external MF. The width and length of the slit are $0.1\lambda_p$ and 300 μm, respectively. The incident frequency is $\omega = 0.6\omega_{ps}$, which is in the one-way-propagating frequency band. The arrows indicate the incident directions. (e) Transmitted intensities of the forward- [corresponding to (c)] and backward-propagating [corresponding to (d)] waves when 1 T MF is applied.

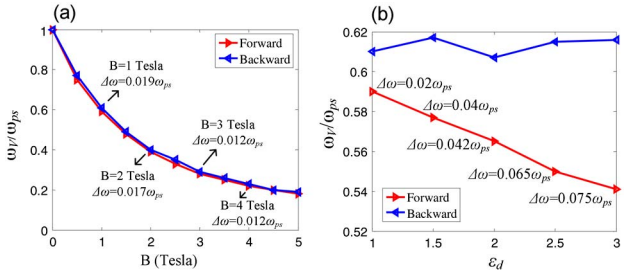

Fig. 3. (Color online) Effects of (a) the external MFs B and (b) the permittivity of the dielectric layer ε_d on the one-way-propagating frequency band. ω_V represents the cutoff frequency. $\Delta\omega = \omega_{Vb} - \omega_{Vf}$ is the bandwidth of the one-way-propagating band.

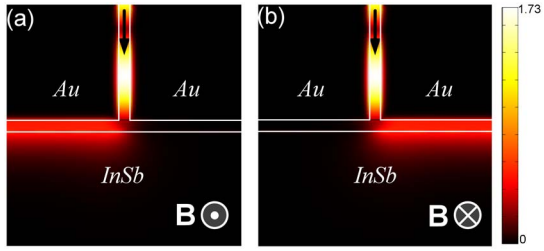

Fig. 4. (Color online) $|H_y|^2$ distributions of a designed THz plasmonic switch tuned by an external MF. (a) The MF direction is along the y axis. (b) The MF direction is along the $-y$ axis.

cutoff frequencies of both the forward- and backward-propagating modes [see Fig. 3(a)]. The cutoff frequencies of the two modes decrease dramatically (from $0.76\omega_{ps}$ to $0.18\omega_{ps}$ corresponding to from 1.5 THz to 0.36 THz) with the increase of the MF (from 0.5 to 5 T). It is interesting to note that the bandwidth of the one-way-propagating band $\Delta\omega$ depends little on the MF. On the other hand, it is mainly determined by the permittivity of the dielectric layer ε_d as seen in Fig. 3(b), where $\Delta\omega/\omega_{ps}$ increases from 0.02 to 0.075 (corresponding to from 0.04 THz to 0.15 THz) as ε_d increases from 1 to 3.

The effects of B and ε_d on the one-way-propagating frequency band can also be explained analytically. By applying the non-retardation limit [15], i.e., $\beta \gg k_0$, into Eq. (3), we have $\kappa_1 \approx \kappa_2 \approx \kappa_3 \approx \beta$, and $\beta w \gg 1$. Thus the cutoff frequencies of the forward- and the backward-propagating modes ω_{Vf} and ω_{Vb} can be expressed as

$$\omega_{Vf} = \frac{1}{2}\left[\sqrt{\omega_c^2 + 4\omega_{ps}^2\varepsilon_\infty/(\varepsilon_d + \varepsilon_\infty)} - \omega_c\right]$$
$$\omega_{Vb} = \frac{1}{2}\left[\sqrt{\omega_c^2 + 4\omega_{ps}^2} - \omega_c\right], \quad (4)$$

respectively. It can be seen that the one-way-propagating bandwidth can be obtained analytically as $\Delta\omega = \omega_{Vf} - \omega_{Vb}$, which increases with ε_d. ω_{Vf} rather than ω_{Vb} is dependent on ε_d because of the asymmetry of the mode distribution caused by the MF. From simulations, the forward-propagating wave is mostly confined on the insulator/semiconductor interface, while the backward-propagating wave is confined on the insulator/metal interface. Because the permittivity of metal is very large ($|\varepsilon_m| \gg \varepsilon_d$), the impact of varying ε_d on the insulator/metal interface is much weaker than on the insulator/semiconductor interface.

Last but not least, we present an application example of this one-way THz waveguide for realizing a THz plasmonic switch. It should be noted that if we change the propagation direction of the applied MF, i.e., from B to $-B$, the dielectric tensor matrix in Eq. (1) will be transposed. As a result, the dispersion relation of the forward- and backward-propagating waves is interchanged, which means the one-way-propagating band will not block the forward wave, but the backward wave. According to this principle, we design a T-shape waveguide, as shown in Fig. 4. The width of the waveguide is $0.1\lambda_{ps}$. The MF intensity is 1 T, and the incident angular frequency is $\omega = 0.6\omega_{ps}$ within the one-way-propagating band. It is clearly seen that when the direction of the external MF is changed, a tunable THz plasmonic switch can be realized.

In conclusion, we present a one-way-propagating THz plasmonic waveguide and a tunable THz plasmonic switch based on the nonreciprocal SMPs. The proposed waveguide structure and the concept may open a new avenue of realizing various tunable THz plasmonic devices.

References

1. I. Hosako, N. Sekine, M. Patrashin, S. Saito, K. Fukunaga, Y. Kasai, P. Baron, T. Seta, J. Mendrok, S. Ochiai, and H. Yasuda, Proc. IEEE **95**, 1611 (2007).
2. M. Belkin, Q. J. Wang, C. Pflugl, A. Belyanin, S. P. Khanna, A. G. Davis, E. Linfield, and F. Capasso, IEEE J. Sel. Top. Quantum Electron. **15**, 952 (2009).
3. I. Duling and D. Zimdars, Nat. Photon. **3**, 630 (2009).
4. V. Berger and C. Sirtori, Semicond. Sci. Technol. **19**, 964 (2004).
5. K. Wang and D. M. Mittleman, Nature **432**, 376 (2004).
6. T. Xu, Y. Zhao, D. Gan, C. Wang, C. Du, and X. Luo, Appl. Phys. Lett. **92**, 101501 (2008).
7. J. Chen, Z. Li, S. Yue, and Q. Gong, Appl. Phys. Lett. **97**, 041113 (2010).
8. J. Brion, R. F. Wallis, A. Hartstein, and E. Burstein, Phys. Rev. Lett. **28**, 1455 (1972).
9. Z. Yu, G. Veronis, Z. Wang, and S. Fan, Phys. Rev. Lett. **100**, 23902 (2008).
10. E. D. Palik and J. K. Furdyna, Rep. Prog. Phys. **33**, 1193 (1970).
11. B. Hu, Q. J. Wang, S. W. Kok, and Y. Zhang, "Active focal length control of terahertz slitted plane lenses by magneto-plasmons," Plasmonics (published online, November 2, 2011).
12. C. R. Williams, S. R. Andrews, S. A. Maier, A. I. Fernández-Domínguez, L. Martín-Moreno, and F. J. García-Vidal, Nat. Photon. **2**, 175 (2008).
13. J. G. Rivas, C. Janke, P. H. Bolivar, and H. Kurz, Opt. Express **13**, 847 (2005).
14. S. Linden, C. Enkrich, M. Wegener, J. Zhou, T. Koschny, and C. M. Soukoulis, Science **306**, 1351 (2004).
15. M. S. Kushwaha and P. Halevi, Phys. Rev. B **36**, 5960 (1987).